Wnt5A Signaling Blocks Progression of Experimental Visceral Leishmaniasis

Shreyasi Maity[1], Arijit Chakraborty[2], Sushil Kumar Mahata[3], Syamal Roy[1], Anjan Kumar Das[4] and Malini Sen[1]*

[1] Cancer Biology & Inflammatory Disorder, CSIR-Indian Institute of Chemical Biology, Kolkata, India, [2] Department of General Surgery, Massachusetts General Hospital, Boston, MA, United States, [3] Medicine, VA San Diego Healthcare System, University of California, San Diego, La Jolla, CA, United States, [4] Department of Pathology Calcutta National Medical College & Hospital, Kolkata, India

Visceral leishmaniasis, caused by *L. donovani* infection is fatal if left untreated. The intrinsic complexity of visceral leishmaniasis complicated further by the increasing emergence of drug resistant *L. donovani* strains warrants fresh investigations into host defense schemes that counter infections. Accordingly, in a mouse model of experimental visceral leishmaniasis we explored the utility of host Wnt5A in restraining *L. donovani* infection, using both antimony sensitive and antimony resistant *L. donovani* strains. We found that Wnt5A heterozygous (Wnt5A +/-) mice are more susceptible to *L. donovani* infection than their wild type (Wnt5A +/+) counterparts as depicted by the respective Leishman Donovan Units (LDU) enumerated from the liver and spleen harvested from infected mice. Higher LDU in Wnt5A +/- mice correlated with increased plasma gammaglobulin level, incidence of liver granuloma, and disorganization of splenic white pulp. Progression of infection in mice by both antimony sensitive and antimony resistant strains of *L. donovani* could be prevented by activation of Wnt5A signaling through intravenous administration of rWnt5A prior to *L. donovani* infection. Wnt5A mediated blockade of *L. donovani* infection correlated with the preservation of splenic macrophages and activated T cells, and a proinflammatory cytokine bias. Taken together our results indicate that while depletion of Wnt5A promotes susceptibility to visceral leishmaniasis, revamping Wnt5A signaling in the host is able to curb *L. donovani* infection irrespective of antimony sensitivity or resistance and mitigate the progression of disease.

Keywords: wnt, leishmaniasis, macrophage, T cell, splenomegaly, white pulp

INTRODUCTION

Visceral leishmaniasis (VL) or Kala-azar is a vector borne disease transmitted by the sand fly and caused by infection with the parasite *Leishmania donovani* (*L. donovani*). *L. donovani* promastigotes delivered to the host during a blood meal by the sand fly differentiate within host macrophages to amastigotes, which replicate in macrophages and build their niche therein at the cost of the host cell machinery. Globally, VL is among the top ten neglected tropical diseases in the World Health Organization list. There are outbreaks of VL in certain pockets in developing countries and the disease if left untreated can turn out fatal [(1–3), https://www.who.int/news-room/fact-sheets/detail/

leishmaniasis]. Although different modes of therapy for VL are available, the increasing emergence of drug resistant strains makes treatment complicated (3–5). In this scenario it is important to understand the intricacies of the host – parasite interactions and how host immunity can be boosted to counter the parasite infection. Keeping in mind the documented role of Wnt5A signaling in the regulation of bacterial infections and immune homeostasis (6–10), we became interested in evaluating the influence of Wnt5A on *L. donovani* infection and progression of VL.

Wnt5A, a secreted glycoprotein belongs to a 19 - member family of Wnt ligands that interact with Frizzled and/or ROR cell surface receptors during signal transduction in cells. On account of considerable homology among the Wnts and the Wnt receptors, overlap exists in the pairing of Wnts with their cognate receptors leading to cross talk among the intracellular intermediates at the different levels of Wnt signaling. Classically, the transcriptional coactivator β-catenin is essential for the canonical mode of Wnt signaling, but in the non-canonical mode of Wnt signaling represented by Wnt5A, β-catenin is dispensable (11–16).

Wnt5A signaling sustains cell differentiation and polarity. This property of Wnt5A signaling is utilized in the maintenance of immune homeostasis, wherein it regulates cytoskeletal actin dynamics during macrophage mediated phagocytosis of microbes and their autophagic clearance (8, 10, 17, 18). In the context of *L. donovani* infection, we previously demonstrated that a Wnt5A-Rac1-Actin axis prevents the growth of *L. donovani* in macrophages by abolishing the sustenance of parasitophorous vacuoles through enhancement of prasitophorous vacuole – lysosome fusions (19). These studies prompted us to investigate the potential of Wnt5A in restraining experimental visceral leishmaniasis caused by *L. donovani* infection in mice.

In the current study we have demonstrated that genetic depletion of Wnt5A in Wnt5A heterozygous mice leads to increased susceptibility to the development and progression of disease upon *L. donovani* infection. Administration of recombinant Wnt5A (rWnt5A) prior to *L. donovani* infection, on the other hand, renders resistance to the development of experimental visceral leishmaniasis. Blockade in disease pathogenesis by Wnt5A signaling may be attributed to T cell and macrophage activation and regulation of cytokine expression.

MATERIALS AND METHODS

Reagents

For cell and parasite culture RPMI 1640 (Cat No. - 31800-022) and Medium 199 (Cat No.-11150-059) were purchased from Gibco, USA. APC rat anti-mouse CD138 (Cat No. - 558626), V500 syrian hamster anti-mouse CD3 (Cat No. - 560771), PerCP-Cy5.5 rat anti-mouse CD4 (Cat No. - 550954), BV605 rat anti-mouse CD8 (Cat No. - 563152) and PE-CF594 rat anti-mouse IFN-γ were purchased from BD Biosciences; PE-Cyanine 7 rat anti-mouse Granzyme B (Cat. No.- 25-8898-82), anti-mouse CD169 (Cat no.-MA516508), anti-mouse CD209b (Cat

no. – 14-2093-82), goat anti-rat IgG secondary Alexa Fluor 488 (Cat no.-A-11006), goat anti-hamster IgG alexa fluor 647 (Cat no. - A-21451) and goat anti-rabbit alexa fluor 488 (Cat No. - A11008) were purchased from eBioscience; anti-mouse F4/80 (Cat No.-SC52664) and anti-IL-4 antibody (SC-1261) was purchased from Santa Cruz; anti-human/mouse Wnt5A monoclonal antibody (Cat no.- MAB645) and anti-rat IgG-HRP (Cat no.- HAF005) were purchased from R & D Systems and anti-rabbit IgG-HRP (Cat no.- A0545) and anti-mouse IgG-HRP (Cat no.- A9044) were purchased from Sigma. Anti-mouse IL-10 ELISA set (Cat no. – 555252) and anti-mouse IFN-γ ELISA set (Cat no. – 555138) were purchased from BD Biosciences. Anti-iNOS antibody raised in rabbit (Cat No.-D6B6S, Cell Signalling Technology) was a kind gift from Dr. Partha Chakrabarti, IICB. 7-AAD viability staining solution (Cat no.-420403) was purchased from Biolegend. Fetal Bovine Serum (Cat no. – 10082147), PenStrep (Cat no.- 15140122), L-Glutamine (Cat no. – 25030081), DAPI (Cat no.-D1306), alexa fluor 555 phalloidin (Cat no. – A34055) and cell tracker green (Cat no.-C2925) were purchased from Invitrogen. Histopaque solution (Cat no.- 10771-100ml) and poly-l-lysine (Cat no.- P-8920) were purchased from Sigma. TMB solution (Cat no.- CL07-1000MLCN) was purchased from Merck. Bradford reagent (Cat no. -5000006) was purchased from Biorad, USA. Recombinant Wnt5A (Cat no.- 10UG 645-WN-010 R & D, GF146 Millipore) and recombinant Wnt3A (Cat no.- 10UG 5036-WN-010 R & D, GF154 Millipore) were purchased from R & D Systems and Millipore. Giemsa stain (Cat No.- S011) was purchased from Himedia. BSA was purchased from SRL (Cat No.- SRL-83803) and DCF-DA was purchased from Calbiochem (Cat No.- CAS 4091-99-0).

Animal Maintenance

BALB/c mice were maintained in institute animal facility. B6;129S7-*Wnt5Atm1Amc*/J mice were purchased from Jackson Laboratory, USA and breeding was done in-house. Genotyping was performed to differentiate Wnt5A wild type from Wnt5A heterozygous mice by following Jackson laboratory protocol [(8), https://www.jax.org/Protocol?stockNumber=004758&protocolID=23556]. Animals were kept in IVC (Individually Ventilated Caging) system with *ad libitum* water and food under optimum physiological temperature and balanced light and dark cycle. All experimental groups comprised mice of 8-12 weeks old.

Parasite and Cell Maintenance

L. donovani WHO reference strain AG83 [MHOM/IN/1983/AG83] and Stibogluconate resistant strain BHU575 [MHOM/IN/2009/BHU575/0] were regenerated from BALB/c mice infected separately with the two different strains. Promastigote form of the parasite was maintained in a B.O.D. shaker incubator at 22°C in Medium 199 supplemented with 20% FBS, 2 mM L-glutamine, 100 U/ml penicillin, and 100 mg/ml streptomycin. Freshly transformed stationary-phase promastigotes were harvested and washed in 0.02 M phosphate buffered saline, pH 7.2 for injection into mice. The BHU575 strain was a kind gift from Dr. Shyam Sundar, BHU, Varanasi, India.

Peritoneal macrophages were isolated from BALB/c mice. The peritoneum was washed with ice-cold PBS for harvesting peritoneal lavage. Then the lavage was centrifuged at 2000 rpm and the peritoneal cells were resuspended in RPMI 1640 medium supplemented with 10% FBS, 2 mM L-glutamine, 100 U/ml penicillin, and 100 mg/ml streptomycin.

Quantification of parasite load in liver and spleen of animals: Each experimental mouse was infected with 10^8 promastigotes through the tail vein and sacrificed either 45 days or 110 days post infection for generating imprints of the infected liver and spleen. For protein pretreatment experiments, each mouse was intravenously injected with 100 ng rWnt5A or 100 ng rWnt3A (in 50 µl PBS) on consecutive days before the infection and subsequent imprint collection. Tissue imprints were fixed in chilled absolute methanol and stained with Giemsa. Giemsa-stained micrographs were captured in the bright field of Leica microscope under 100X magnification with a Leica DFC450c camera. LDU calculation was done based on at least 30 microscopic fields by counting the number of amastigotes per 1000 host nuclei and multiplying by respective organ weight in gram (20).

Tissue Histology and Histological Scoring

Tissue histology was performed following published protocols (21). Mouse spleen and liver was dissected out and fixed in 10% buffered formalin overnight. Following dehydration in graded alcohol, each paraffin embedded tissue was sectioned using a microtome at a thickness of 3 µ, subsequent to which the sections were mounted in Mayer's albumin-coated glass slides and stained with hematoxylin–eosin for microscopic analysis.

In H & E-stained spleen tissue sections histological scoring was done following previously published protocol with minor modifications (22). The degree of white pulp structural organization was evaluated based on 4 different criteria: well organized (OD: distinct germinal centre and marginal zone), slightly disorganized (SD: slight loss in distinctness of germinal center and marginal zone), moderately disorganized (MD: poorly individualized or indistinct germinal center and marginal zone) and intensely disorganized (ID: distinctness of white pulp from the red pulp area barely visible). In each case, the percent organization of the spleen in terms OD, SD, MD and ID was assessed by dividing the number of white pulps under each category by the total number of countable white pulps (from at least 10 fields per mouse) and multiplying the ratio by 100. For liver histological scoring, using H & E stained liver tissue sections the total number of granulomas were counted from at least 20 microscopic fields per mouse.

Flow Cytometry

Single cell suspensions generated from mouse spleen (teasing harvested spleen on mesh and collection of cells through strainer), and PBMC harvested from mouse cardiac blood (https://www.infinity.inserm.fr/wp-content/uploads/2018/01/PBMC-isolation-and-cryopreservation.pdf) were subjected to analysis by flow cytometry. Depending upon the purpose of the experiment, cells were surface stained separately for 1 hour at 4°C with different antibodies: anti-CD138-APC (for plasma cell),

anti-F4/80-FITC (for macrophage), anti-CD169 and anti-rat Alexa fluor 488 (for marginal metallophillic macrophage), anti-CD3-HorizonV500 (for CD3), anti-CD4-PerCPCy5.5 (for CD4) and anti-CD8-BV605 (for CD8). Subsequently, cells were washed and processed for analysis. For both intracellular and surface staining, splenocytes were plated and incubated overnight under normal tissue culture conditions with Brefeldin A (3µg/mL) during the last 4 hours of incubation. Subsequently, cells were fixed with 1% paraformaldehyde and permeabilized using permeabilization buffer (0.1% Tween 20 + 1% BSA in 1X PBS) before finally staining with anti-CD3-HorizonV500, anti-CD4-PerCPCy5.5, anti-CD8-BV605, anti-IFN-γ-PE-CF594 and anti-Granzyme-B-PE-Cy7. For checking viability, splenocytes were separately kept under experimental conditions pertaining to the study and stained with 7-AAD for 10 minutes prior to fixation (as a reference for T cell analysis) or before data acquisition (as a reference for macrophage analysis). Data acquisition was done in BD.LSR Fortessa Cell analyser. Data was analyzed using FCS express 5 software. Gating strategies are explained in the **Supplementary Figures**.

Confocal Microscopy

Tissue sections, processed as described before were mounted on poly-L-lysine-coated glass slides for immunofluorescence microscopy following standard protocol (23, 24). The prepared slides were immersed in sodium citrate buffer [10 mM sodium citrate, 0.05% Tween 20 (pH 6.0)] and placed in a pressure cooker for heat-induced antigen retrieval. The slides were then incubated with primary antibody (anti-mouse CD209b antibody) overnight at 4°C after blocking with 10% normal serum and 1% BSA in TBS (Tris Buffered Saline). A fluorophore-conjugated secondary antibody (anti-hamster 2° antibody alexa fluor 647 conjugated) followed by DAPI (nuclear stain) was used to detect the signal under 40X magnification of TCS-SP8 confocal microscope.

Peritoneal exudate was collected from BALB/c mice and plated for 6 hours. The peritoneal macrophages were treated with either PBS (vehicle control) or rWnt5A for 6 hours followed by infection with cell tracker green stained *L. donovani* AG83 promastigotes for 4 hours at 5 MOI and washed 3 times with chilled 1X PBS, following which incubation was continued for 12 hrs in fresh culture medium. Subsequently the cells were fixed in 4% paraformaldehyde for 15 min, and Phalloidin and DAPI staining was done for 15 minutes using Alexa Fluor 555 Phalloidin (1:2,000) and DAPI (1:4,000) in PBST (0.1% Tween-20) containing 2.5% BSA. Following 3X PBST wash, the slides were mounted with 60% glycerol and visualized under 63X magnification (2.51 zoom) of TCS-SP8 confocal microscope.

Transmission Electron Microscopy

Thin slices (~2 mm thick) of *L. donovani* infected mouse spleen and liver were immersion fixed with 2% glutaraldehyde in 0.1 M cacodylate buffer and postfixed further with 1% OsO_4 in 0.1 M cacodylate buffer on ice for 1 hr. The fixed tissue was stained with 2% uranyl acetate for 1 hr on ice, after which it was dehydrated in graded series of ethanol (50-100%) while remaining on ice. The fixed dehydrated tissue was subjected to 1 wash with 100%

ethanol and 2 washes with acetone (10 min each) and finally embedded with Durcupan. Subsequently, sections were cut at 60 nm on a Leica UCT ultramicrotome, and mounted on Formvar and 300 mesh copper grids. Subsequently, the sections were stained with 2% uranyl acetate for 5 minutes and Sato's lead stain for 1 minute. Finally, grids were viewed using a JEOL JEM1400-plus transmission electron microscopy (TEM) (JEOL, Peabody, MA) and photographed using a Gatan OneView digital camera with 4×4k resolution (Gatan, Pleasanton, CA).

Mouse Cytokine and Anti-Leishmanial IgG Estimation

IL-10 and IFN-γ of mouse plasma was measured with BD ELISA Set (catalog numbers 555138 and 555252 for IFN-γ and IL-10 respectively) following manufacturers protocol (www.bdbiosciences.com). Briefly 96 well polystyrene ELISA plates were coated with capture antibody and kept at 4°C overnight. After washing with PBST, plates were blocked with 10% FBS in 1X PBS for 1 hour. Following the addition of 100 ml of 1:10 diluted plasma samples, the plates were incubated with biotinylated detection antibody and streptavidin HRP. Subsequently TMB was added and Stop solution (2N H_2SO_4) was used after 30 minutes to stop the color reaction. Reading was taken at 450 nm in an ELISA plate reader. The level of IL-4 was estimated from 100 μl of 1:10 diluted plasma samples, plated on 96 well polystyrene ELISA plates overnight at 4°C. After 3X wash with PBST, plates were blocked with 1% BSA (Bovine Serum Albumin) for 2 hours. Then the plates were probed with anti-IL-4 antibody (1:1500 dilution) raised in goat. After overnight incubation at 4°C, plates were washed with PBST following which incubation with HRP conjugated anti-goat IgG (1:8000 dilution) for 2 hours was performed. Subsequently TMB (HRP substrate) was added and stop solution (2N H_2SO_4) was used after 30 minutes to stop the colour reaction. Reading was taken at 450 nm in an ELISA plate reader.

Anti-Leishmanial IgG estimation was performed following previously published protocol (25). Briefly, stationary-phase promastigotes of *L. donovani* AG83 and *L. donovani* BHU575 were harvested for antigen preparation. After 4X wash with ice-cold PBS, the parasite pellet was suspended at a concentration of about 1.0 g of pellet in 50 ml of cold 5 mM Tris-HCl buffer, pH 7.6. Subsequently, after short spans of intermittent vortexing and incubations on ice and a 10 min centrifugation at 2310Xg the resultant remnant membrane pellet was suspended in Tris buffer of the same pH and sonicated multiple times with occasional incubations on ice. Following a final 30 min centrifugation at 4390Xg, the supernatant which contained the leishmanial antigen (LAg) was carefully harvested and stored as frozen aliquots until further use in ELISA. For ELISA, plates were first coated with 20μg/ml of LAg in PBS and left overnight at 4°C. Subsequently, after several washes with PBS-0.05% Tween 20, blocking with 1% BSA and further washes at room temperature, mouse plasma samples (1:100 dilution in PBS with 1% BSA) were added to the different antigen coated wells and incubation was continued overnight at 4°C. After routine washing, incubation with HRP conjugated anti-mouse IgG goat polyclonal antibody (1: 10,000 dilutions in PBS) was continued for about 3 hrs at

room temperature. TMB substrate was applied after washing for color development and following the addition of stop solution, reading was taken at 450 nm using ELISA plate reader.

Estimation of Wnt5A in Mouse Plasma

The level of Wnt5A was estimated from mouse plasma samples. 100μl of 1:10 diluted plasma samples were plated on 96 well polystyrene ELISA plates overnight at 4°C. After 3X wash with PBST, plates were blocked with 1% BSA (Bovine Serum Albumin) for 2 hours. Then the plates were probed with anti-human/mouse Wnt5A antibody (1:1000 dilution) raised in rat. After overnight incubation at 4°C, plates were washed with PBST following which incubation with HRP conjugated anti-Rat IgG (1:4000 dilution) for 2 hours was performed. Subsequently TMB (HRP substrate) was added and stop solution (2N H_2SO_4) was used after 30 minutes to stop the colour reaction. Reading was taken at 450 nm in an ELISA plate reader.

Estimation of Wnt5A in Human Plasma

Human samples were collected from Murarai village, Birbhum, WB, India. Samples were tested for rK39 in Malaria Clinic, Calcutta School of Tropical Medicine, India. For estimating the Wnt5A level in human plasma samples, 96 well ELISA plates were coated with plasma samples (1:50 dilution) overnight at 4°C. After 3X wash with PBST, plates were blocked with 1% BSA for 2 hours. Then the plates were incubated overnight at 4°C with anti-human/mouse Wnt5A antibody (1:2000 dilution) raised in rat. After washing with PBST, incubation with HRP conjugated anti-Rat IgG (1:4000 dilution) was continued for 2 hours. Subsequently TMB was added for developing color and stop solution (2N H_2SO_4) was used after 30 minutes to stop the colour reaction. Reading was taken at 450 nm in an ELISA plate reader.

Estimation of ROS

The fluorescent probe H2DCF-DA was used to check accumulated ROS production in the spleen of Wnt5A+/+ and Wnt5A+/- mice or in rWnt5A/rWnt3A/PBS(VC) pretreated BALB/c mice. Single cell suspension was made from the spleens harvested from mice under each category. Cells were incubated with H2DCF-DA (10 μM) for 20 minutes at 37°C in a CO_2 tissue culture incubator. Subsequently, the cells were washed three times with PBS and data acquisition was done in BD.LSR Fortessa Cell analyser. Data was analyzed using FCS express 5 software.

Estimation of iNOS

For checking the level of iNOS, peritoneal exudate collected from BALB/c was plated for 10 hours. The macrophages were treated with either PBS (vehicle control) or with rWnt5A/rWnt3A (50 ng/ml) for 6 hours followed by infection with *L. donovani* AG83 at 5 MOI for 4 hours. After washing with PBS, incubation was continued for 12 hours in fresh medium. Subsequently cells were fixed in 4% paraformaldehyde for 10 minutes, permeabilized with 0.1% Triton X-100 for 10 minutes and blocked with 3% BSA for 2 hours at room temperature. Cells were then incubated with anti-mouse iNOS antibody (1:400) at 4°C overnight. Alexa fluor 488 conjugated goat anti-rabbit secondary antibody (1:500)

followed by DAPI (1:4000) counterstain was used to detect iNOS under 63X magnification (oil immersion) of Leica TCS-SP8 confocal microscope. Mean fluorescence intensity per field was measured using ImageJ software.

Statistical Analysis

The data were analyzed by Graph Pad Prism 5 software using unpaired t test. Scatter plots and bar graphs are expressed as mean ± SEM. $p \leq 0.05$ was considered statistically significant. Significance was annotated as follows: *$p \leq 0.05$, **$p \leq 0.005$, ***$p \leq 0.0005$, ns: not significant.

RESULTS

Disease from *L. donovani* Infection is More Pronounced in Wnt5A Heterozygous Mice than in the Wild Type Counterparts

In view of the fact that Wnt5A signaling antagonizes *L. donovani* infection in macrophages (19) we wanted to examine if Wnt5A signaling regulates the progression of experimental visceral leishmaniasis. Accordingly, we evaluated the effect of genetic depletion of Wnt5A on the progression of the disease using a mouse model. In essence, we assessed the intensity and outcome of *L. donovani* infection in Wnt5A heterozygous (H: Wnt5A+/-) mice of B6:129S7 origin (https://www.jax.org/strain/004758), as compared to the wild type (W: Wnt5A+/+) counterparts. On account of the prevalence of different strains of *L. donovani*, with different degrees of drug sensitivity or resistance, we used two strains of the parasite, AG83 (antimony sensitive) and BHU575 (antimony resistant), for our study. The aim was to evaluate the influence of host Wnt5A on the two different *L. donovani* strains independent of their drug sensitivity or resistance. Validation of genetic depletion of Wnt5A in the Wnt5A heterozygous mice and the decreased level of the Wnt5A protein therein as compared to that in the wild type is depicted in **Figure S1**.

Estimation of *L. donovani* infection in liver and spleen: Leishman Donovan Units (LDU) enumerated from imprints of infected liver and spleen of both sets of mice sacrificed either 45 days or 110 days after infection with either AG83 or BHU575 revealed that liver and spleen of the Wnt5A heterozygous mice harbored significantly greater number of parasites as compared to those of the wild type controls (**Figure 1A**). Augmented parasite abundance in the heterozygous mice as compared to the wild type was corroborated by light microscopy of Giemsa-stained imprints of the infected liver and spleen (**Figure S2**, Panel A). Consistent with published literature (26), infection in the liver tended to be resolved with the passage of time through 110 days. However, infection prevailed in the spleen, especially in most of the Wnt5A heterozygous mice even after 110 days. Parasitophorous vacuoles were more frequent (shown by red arrowhead) in the spleens of Wnt5A heterozygous mice in comparison to wild type, as demonstrated by TEM (**Figure 1B**).

Spleen Pathology: Increased level of *L. donovani* infection in the Wnt5A heterozygous mice as compared to the wild type

correlated with greater severity of disease as revealed by the prevalence of significantly more disrupted splenic white pulps in the heterozygous mice in comparison to the wild type mice through tissue histology. Upon careful scoring of the levels of organization of splenic white pulps (clearly explained in Materials & Methods under "Tissue histology and histological scoring"), we noted that while the number of organized white pulps was always significantly more in the wild type mice than in the heterozygous mice, the number of moderately to intensely disorganized white pulps was always more in the heterozygous mice than in the wild type (**Figure 2A, B**). The difference in the numbers of slightly disorganized white pulps between the two sets of mice was not found to be significant. Panel A depicts representative micrographs of spleen sections of uninfected and infected mice with different degrees of white pulp organization/disorganization and Panel B is a graphical representation of the degrees of white pulp organization/disorganization in the two sets of mice after parasite infection. Higher numbers of CD138^{+} plasma cells in the spleens of the heterozygous mice, which correlated with increased level of circulating *L. donovani* membrane antigen reactive gammaglobulin (IgG) furthermore, confirmed the disease intensity, as consistent with contemporary literature (**Figures 2C, D**) (25–28). The average size of spleen and its weight per unit weight of body was also considerably more in the Wnt5A heterozygous mice following infection with either AG83 or BHU575, as compared to the control, confirming increased infection induced splenomegaly therein (**Figure S2**, Panels B, C).

Liver pathology: Transmission electron micrographs of liver sections generated 45 days after *L. donovani* infection revealed increased infiltration of monocyte derived macrophages with consequent liver hyperplasia in the Wnt5A heterozygous mice as compared to the wild type controls (**Figures 3A, B**), which is in compliance with the correlation of monocyte/macrophage infiltration with active disease (29, 30). Augmented disease in the Wnt5A heterozygous mice as compared to the wild type was furthermore indicated by the increased incidence of liver granuloma 45 days after *L. donovani* infection as revealed by histology (**Figures 3C, D**) (26).

Overall, our results based on careful evaluation of infected liver and spleen imprints, tissue sections and electron micrographs indicated that both the antimony sensitive AG83 and the antimony resistant BHU575 *L. donovani* strains are more infective in Wnt5A depleted condition. In essence, Wnt5A heterozygous mice, which retained relatively low level of Wnt5A after infection (**Figure S2**, Panel D), developed more intense disease after *L. donovani* infection as compared to the wild type controls. These observations led us to investigate if revamping Wnt5A signaling prevents the development/progression of experimental visceral leishmaniasis.

Administration of Recombinant Wnt5A (rWnt5A) Restrains *L. donovani* Infection and the Progression of Disease Caused by It

In order to evaluate the influence of Wnt5A signaling on experimental visceral leishmaniasis in mice, we examined if the
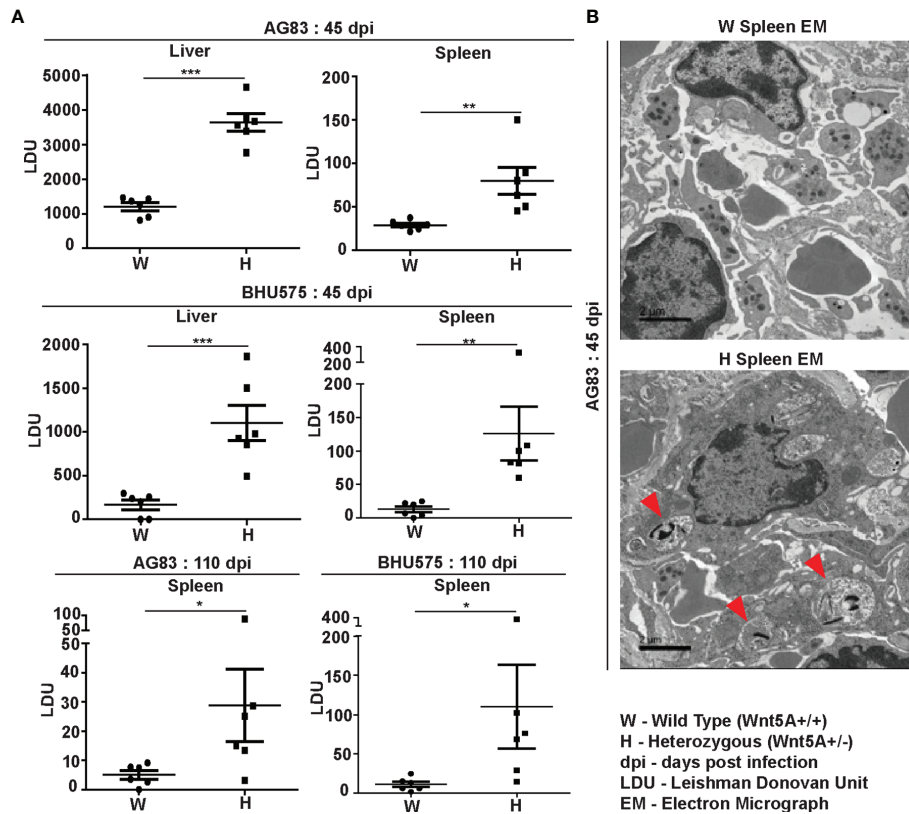
FIGURE 1 | Evaluation of *L. donovani* infection in the liver and spleen of Wnt5A+/+ wild type (W) and Wnt5A+/- heterozygous (H) mice. **(A)** Microscopic examination of imprints of liver and spleen from infected mice reveals significantly higher parasite load as measured by Leishman Donovan Unit (LDU) in the H category of mice than the control W category, both 45 days and 110 days post infection (dpi) with either the AG83 or BHU575 strain of *L. donovani*. **(B)** TEM micrographs showing parasitophorous vacuoles (PV) in a spleen section of H but not W category after infection. PV was more frequent in H than in W. Data are presented as mean ± SEM. Statistical analysis was performed with the unpaired t-test. Significance was annotated as follows: *$p \leq 0.05$, **$p \leq 0.005$, ***$p \leq 0.0005$, n=6 (per group). EM representation is based on evaluation of at least 10 different fields.

administration of recombinant Wnt5A (rWnt5A) is efficacious in preventing *L. donovani* infection and the progression of disease. For our disease model, rWnt5A (100 ng protein in 50 µl PBS) was administered intravenously through the tail vein of BALB/c mice on two consecutive days before infection with 10^8 *L. donovani* promastogotes (either AG83 strain or BHU575 strain) through the same route, and PBS was used as the vehicle control for rWnt5A. Administration of rWnt3A (100 ng protein in 50 µl PBS) was considered as an additional negative control for this study. All infected mice pretreated separately with rWnt5A, rWnt3A or vehicle control were sacrificed either 45 days or 110 days post infection for enumeration of liver and spleen LDU, and evaluation of liver and spleen architecture by histology, following the same procedures described before. In compliance with the results obtained with Wnt5A heterozygous and wild type mice, we found that prior injection of rWnt5A but not rWnt3A or just the vehicle control (PBS) in BALB/c mice inhibits both the degree of infection with *L. donovani* and the progression of disease. As demonstrated in **Figure 4A** both liver and spleen LDU were on average considerably less in the

rWnt5A treated mice as compared to the PBS and rWnt3A administered controls, both in case of AG83 and BHU575 infection. Giemsa stained representative imprints of infected liver and spleen used for LDU evaluation are depicted in **Figure 4B** of the same figure.

In agreement with the trend of LDU values obtained from splenic imprints, spleens of the *L. donovani* (AG83 or BHU575) infected mice pretreated with rWnt5A revealed preservation of white pulp organization much unlike those of mice treated with only PBS or rWnt3A, where marked disorganization of white pulps was observed. The histological analysis and scoring of white pulp organization in the different sets of mice, which was performed in the same way as described in the previous section is depicted in **Figures 5A, B**. **Figure 5A** illustrates examples of organized (OD), slightly disorganized (SD), moderately disorganized (MD) and intensely disorganized (ID) splenic white pulps from the different sets of mice and Panel B is a graphical representation of the degrees of organization/disorganization therein. Overall, the rWnt5A regimen correlated with the highest numbers of organized and lowest
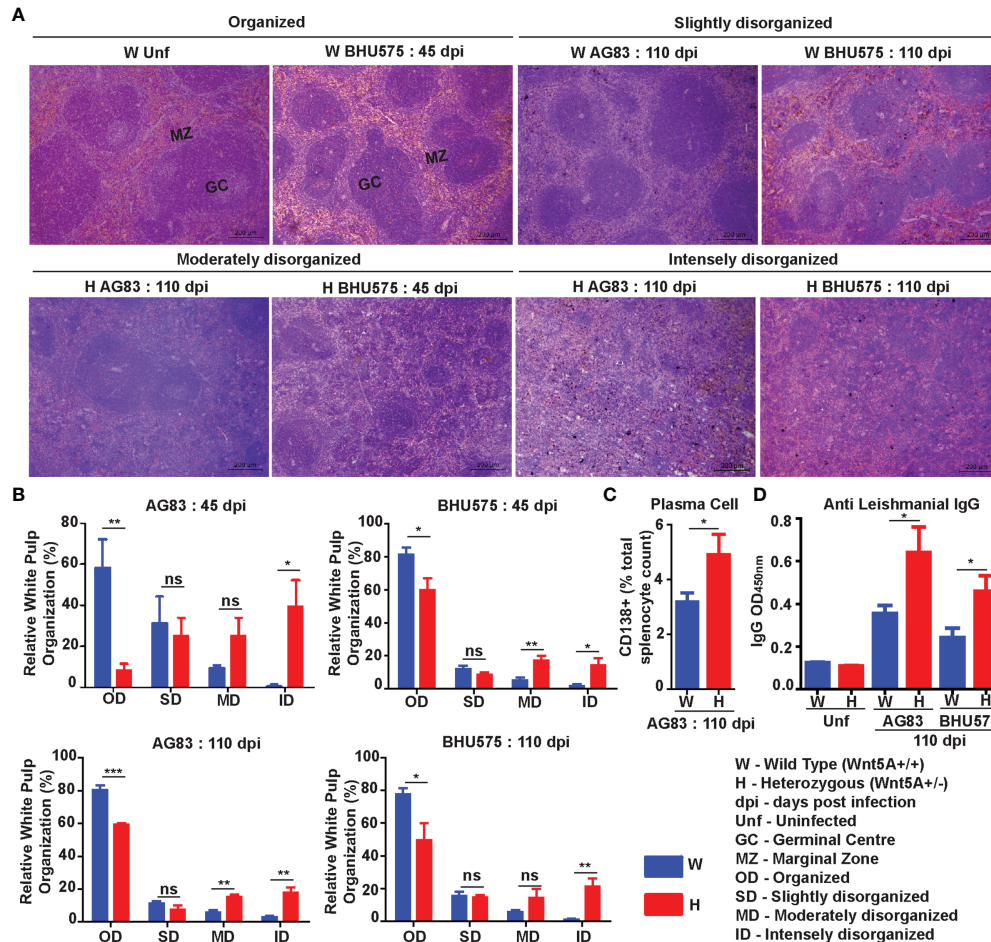
FIGURE 2 | Assessment of spleen pathology in Wnt5A+/- (H) in comparison to Wnt5A+/+ (W) mice after *L. donovani* infection. **(A)** Micrographs (under 10X objective) of representative Hematoxylin & Eosin-stained spleen sections from W and H categories, both before (unf) and after *L. donovani* infection (45 and 110 dpi), depicting different levels of disorganized splenic white pulp as compared to organized (explained in Materials and Methods). **(B)** Graphical representation of different levels of splenic white pulp disorganization in H mice as compared to W, following infection with either AG83 or BHU575, 45 and 110 dpi. **(C, D)** Graphical representation of higher percentage of plasma cells **(C)** and increased levels of IgG **(D)** in H as compared to W, 110 dpi. Statistical analysis was performed with the unpaired t-test. Data are presented as mean ± SEM. Significance was annotated as follows: $*p \leq 0.05$, $**p \leq 0.005$, $***p \leq 0.0005$, ns, not significant, n=4 to n=6 (per group).

numbers of moderately to intensely disorganized white pulps as compared to the other two regimens. Significantly lower numbers of CD138^{+} plasma cells in the spleens of rWnt5A pretreated infected mice as compared to the corresponding controls (PBS and rWnt3A pretreated) matched with the observed intactness of the splenic white pulps (**Figure 5C**). This was in compliance with the relatively low levels of circulating antileishmanial IgG in the rWnt5A treated set **Figure 5D**). Preservation of splenic architecture by rWnt5A treatment was furthermore revealed by blockade of splenomegaly that was induced by *L. donovani* infection (**Figure S3**). The inhibitory effect of rWnt5A on *L. donovani* infection was also evident from the very low numbers of liver granulomas in the rWnt5A treated infected mice as compared to the controls (PBS and rWnt3A treated), where parasites were visible inside the granuloma (**Figure S4**).

Inhibition of Progression of Experimental Visceral Leishmaniasis by Wnt5A Is Associated With an Altered Profile of Macrophages, T Cells and Secreted Cytokines

In view of the documented role of Wnt5A signaling in macrophage and T cell activation (6–10, 19, 31, 32) we examined if the Wnt5A mediated inhibition of disease progression in mice by *L. donovani* infection is linked with changes in the status of macrophages, T cells and cytokines. In essence, we evaluated the immune potential of rWnt5A in relation to rWnt3A and the vehicle control (vc), toward restriction of disease progression.

Flow cytometry performed on splenocytes harvested from the different experimental sets of rWnt5A/rWnt3A/vc pretreated *L. donovani* infected BALB/c mice revealed that the rWnt5A
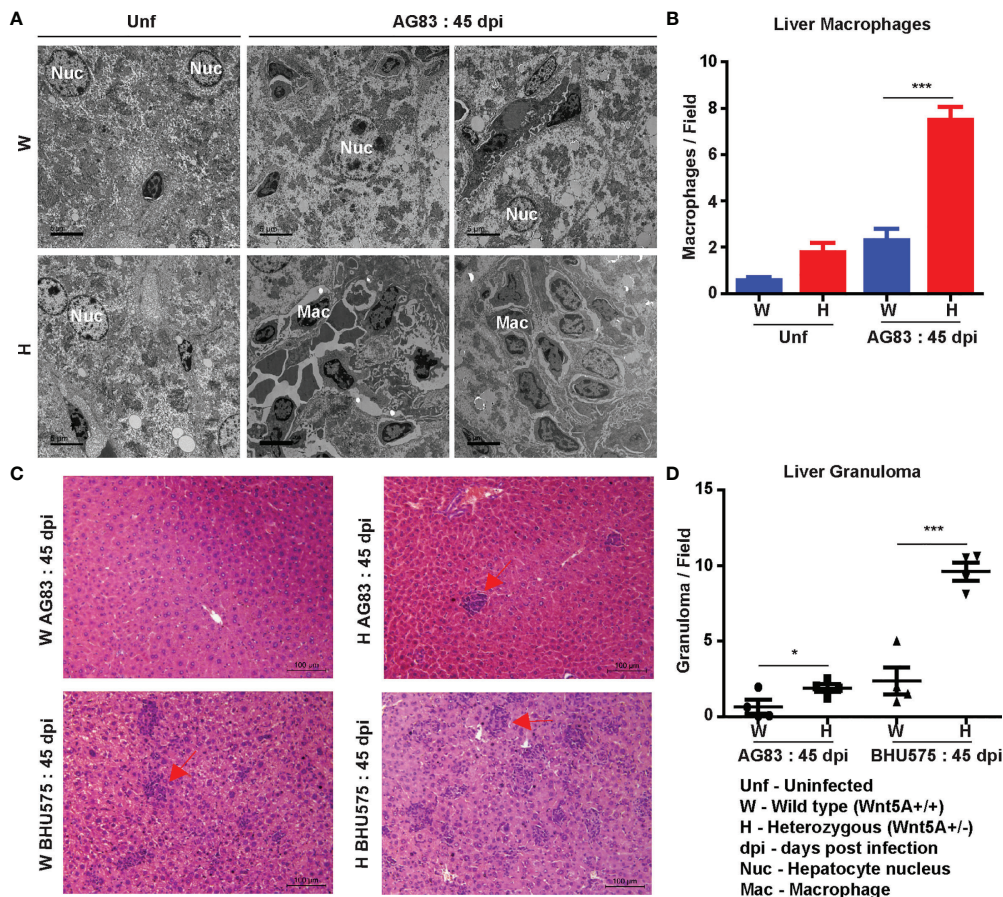
FIGURE 3 | Evaluation of liver pathology of H and W mice after *L. donovani* infection by transmission electron microscopy and histology. **(A, B)** TEM micrographs **(A)** and morphometric analysis **(B)** demonstrating increased numbers of monocytes/macrophages in the liver of H as compared W, 45 dpi. 'Uninfected' (Unf) from each category is used as reference. **(C, D)** Representation of liver granuloma (under 20X objective) in H as compared to W, 45 dpi as demonstrated by histology. Statistical analysis was performed with the unpaired t-test. Data from 10-20 fields are presented as mean ± SEM. Significance was annotated as follows: *$p \leq 0.05$, ***$p \leq 0.0005$. n=4 (per group).

pretreated mice harbored on average higher percentage (percent of counted splenocytes) of activated splenic CD3+CD4+ and CD3+CD8+ T cells, positive for both intracellular IFN-γ and granzyme B (GrB) as compared to those pretreated with just vc or rWnt3A (**Figure 6A**). PBMC harvested from these mice exhibited a similar trend in the percent (percent of counted PBMC) of CD3+CD4+ and CD3+CD8+ T cells (**Figure 6B**). In concurrence with these observations, we noted that the percentage of CD3+CD4+ and CD3+CD8+ T cells in *L. donovani* infected Wnt5A heterozygous mice was considerably less than that in the corresponding wild type controls (**Figure 6C**). Representative examples of our analysis are depicted as FACS dot plot in the respective panels. Since Wnt5A regulates hematopoiesis (33), we questioned if the lower percentage of T cells in the Wnt5A heterozygous mice could be a result of heterozygosity, but did not note any major difference in T cell percentages between the Wnt5A wild type and heterozygous mice (**Figure S5**). Nevertheless, given the

limited sample size tested, heterozygosity as a contributory factor for the low T cell percentages in infected mice perhaps cannot be totally ruled out. The FACS gating strategy and occurrence of minimal cell death during assay is explained in **Figure S6**.

In association with our observation of the Wnt5A dependent prevalence of splenic CD4 and CD8 T cells in the backdrop of *L. donovani* infection, we demonstrated that Wnt5A pretreatment of *L. donovani* infected mice led to a moderately increased presence of CD169+ marginal metallophillic macrophages (MMM), which are known to engulf pathogens, and collaborate with white pulp dendritic cells for antigen presentation to T cells (**Figure 7A**) (34, 35). Additionally, as shown by confocal microscopy, Wnt5A associated MMM abundance was coupled with a structured occurrence of CD209+ marginal zone (MZ) macrophages, also known for their ability to internalize and destroy pathogens (**Figure 7B**) (36). Such profile of MMM and MZ macrophages was not
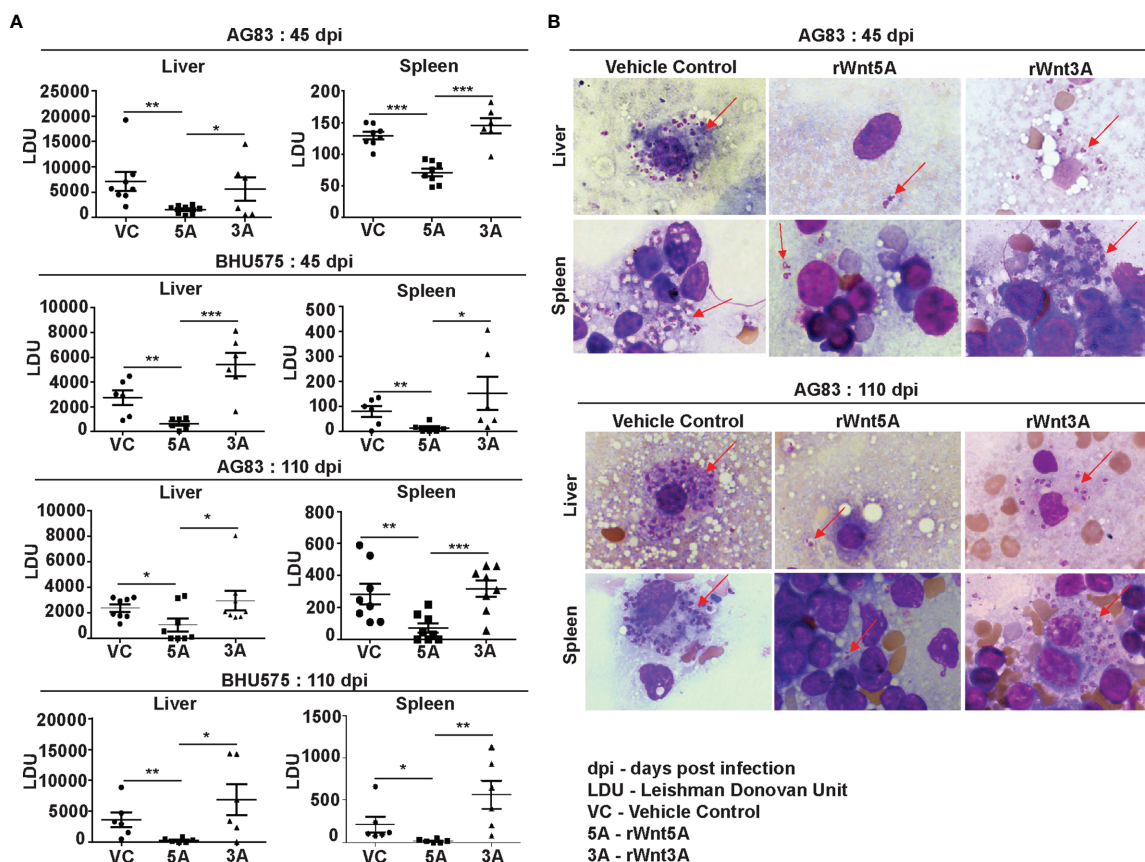
FIGURE 4 | Treatment of mice with rWnt5A restricts *L. donovani* infection. **(A)** Graphical representation of significantly less parasite load (LDU) in spleen and liver imprints of rWnt5A but not rWnt3A pretreated BALB/c mice as compared to corresponding vehicle control (VC: PBS), both 45 and 110 days after infection with either AG83 or BHU575. **(B)** Representative micrographs of Giemsa stained imprints (under 100X objective/oil immersion) of liver and spleen of mice pretreated with rWnt5A, rWnt3A or VC; arrows denoting parasites. Statistical analysis was performed with the unpaired t-test. Data are presented as mean ± SEM. Significance was annotated as follows: *$p \leq 0.05$, **$p \leq 0.005$, ***$p \leq 0.0005$. n=6 to n=8 (per group).

observed in case of pretreatment of the infected mice with rWnt3A or vc (**Figures 7A, B**). In both vc and rWnt3A treated sets, there were relatively lesser percentages of CD169^{+} MMM and absence of a structured organization of CD209b^{+} MZ. Furthermore, as demonstrated by flow cytometry rWnt5A pretreated mice infected with *L. donovani* also harbored increased percentages of F4/80[+] red pulp macrophages, known for their microbe scavenging property (36), in comparison to the vc and rWnt3A pretreated controls (**Figure 7C**).

Wnt5A signaling supported a IFN-γ associated proinflammatory cytokine bias, which is known to antagonize *L. donovani* infection (37) in conjunction with the preservation of splenic T cells and macrophages. Evaluation of the cytokine profile of blood plasma of both Wnt5A+/+ and Wnt5A+/- mice infected with *L. donovani* (either AG83 or BHU575) revealed considerably higher IFN-γ/IL-10 ratio in the plasma samples of Wnt5A+/+ mice in comparison to those of the Wnt5A+/- mice (**Figure 8A**).

Revamping of Wnt5A signaling by rWnt5A treatment before *L. donovani* infection, furthermore, correlated with increased plasma IFN-γ/IL-10 ratio. This was not observed when rWnt3A or vehicle control (vc) was used as a reference for rWnt5A (**Figure 8B**). Administration of rWnt5A prior to infection was also found to correlate with slightly lower plasma levels of IL-4 (**Figure S7**), which may act together with IL-10 to aggravate disease pathogenesis (38).

Altogether, these results suggest that the altered status of splenic macrophages and T cells, and the IFN-γ linked proinflammatory cytokine bias associated with Wnt5A signaling support parasite clearance and help restrict disease progression in experimental visceral leishmaniasis. The augmented levels of Wnt5A dependent ROS and iNOS, demonstrated separately in the spleens of infected mice (**Figures S8A–C**) and in isolated macrophages after infection (**Figures S8D, E**) are in concurrence with parasite killing linked with Wnt5A signaling (1, 26, 37).
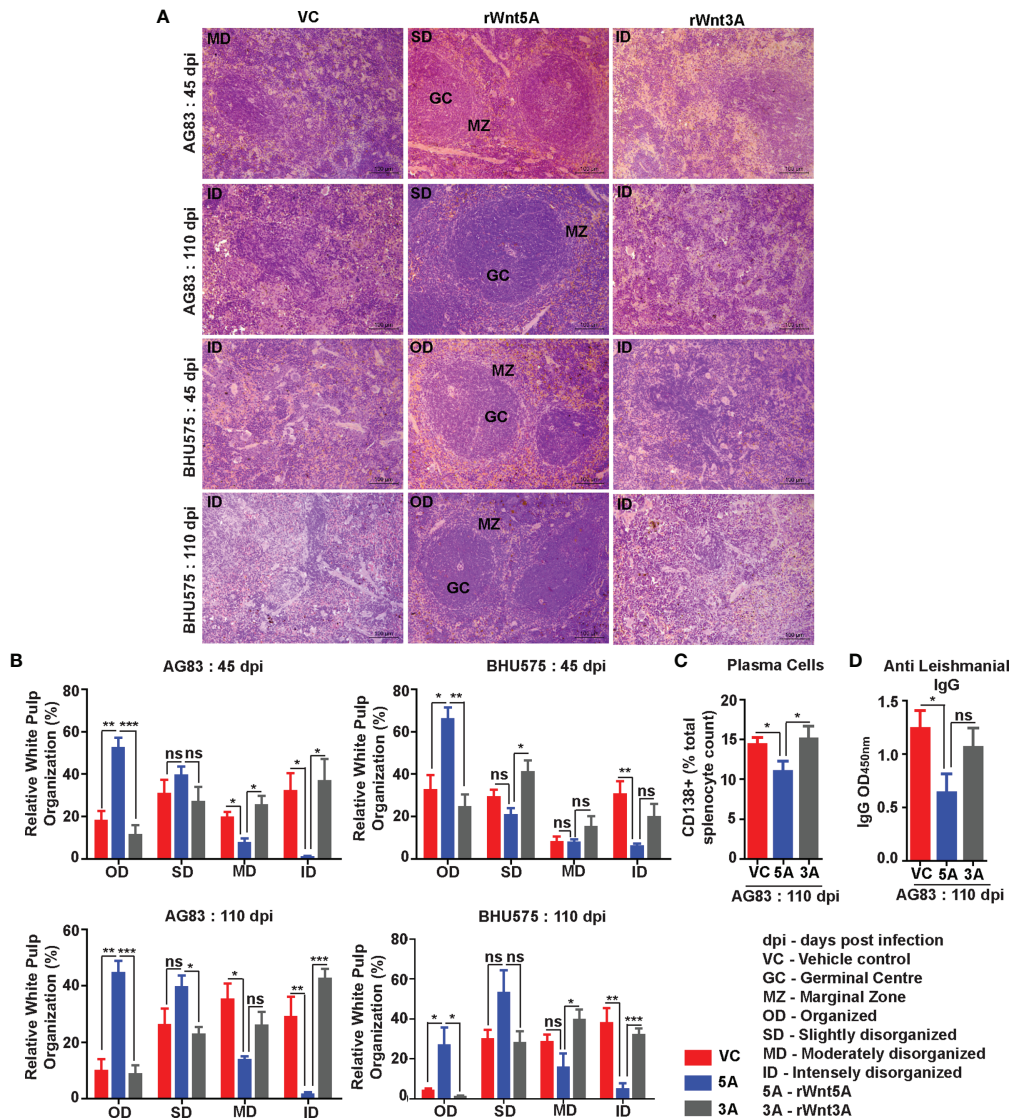
FIGURE 5 | Treatment of mice with rWnt5A inhibits *L. donovani* infection induced disorganization of splenic white pulp. **(A)** Representative micrographs of Hematoxylin & Eosin stained sections of spleen (under 20X objective) depicting significantly less disorganization in splenic white pulp subject to rWnt5A, but not rWnt3A or VC treatment, prior to AG83 or BHU575 infection. **(B)** Graphical representation of extent of preservation of splenic white pulp organization by rWnt5A treatment before infection as compared to rWnt3A or vehicle control. **(C, D)** Graphical representation of lower percentage of CD138+ plasma cells **(C)** and lower level of anti-leishmanial IgG **(D)** in rWnt5A pretreated infected mice as compared to those pretreated with rWnt3A or VC. Data are presented as mean ± SEM. Statistical analysis was performed with the unpaired t-test. Significance was annotated as follows: *$p \leq 0.05$, **$p \leq 0.005$, ***$p \leq 0.0005$. ns, not significant, n=4 to n=6 (per group).

DISCUSSION

In this study we evaluated the potential of Wnt5A signaling in restraining disease progression in a mouse model of experimental visceral leishmaniasis using both antimony sensitive (AG83) and antimony resistant (BHU575) strains of *L. donovani*. We demonstrated that depletion of Wnt5A in Wnt5A heterozygous mice increases susceptibility to experimental visceral leishmaniasis following infection with either AG83 or BHU575 (**Figures 1–3**). Electron micrographs

of mouse liver and spleen sections clearly revealed higher incidence of infiltrating macrophages and increased prevalence of parasitophorous vacuoles, in compliance with higher liver LDU counts and spleen LDU counts respectively, in the heterozygous mice as compared to the corresponding wild type cohorts (**Figures 1**, **3**). Greater disease severity in the heterozygous mice as compared to the wild type was also evident from their relatively increased frequency of disorganized splenic white pulp and splenomegaly (**Figure 2** and **Figure S2**). Administration of rWnt5A, however, helped to
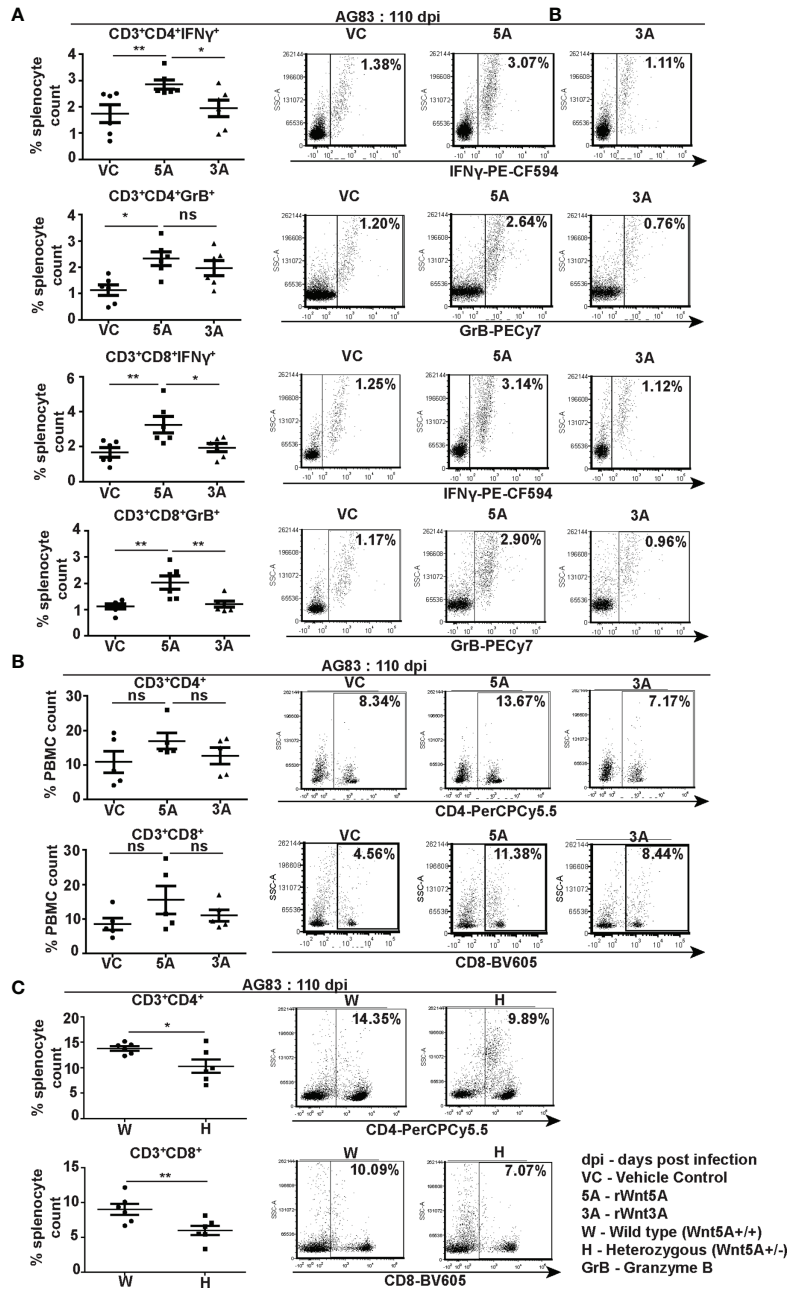
FIGURE 6 | Wnt5A supports CD4 and CD8 T cell maintenance and activation in the backdrop of *L. donovani* infection. **(A)** Graphical representation with specific examples depicted as facs dot plots of increased percentage of IFN-γ positive and GrB positive splenic CD3+CD4+ and CD3+CD8+ T cells subject to rWnt5A treatment before infection, in comparison to the corresponding controls, as depicted by FACS. **(B)** Representation of a similar trend in the PBMC harvested from the same sets of mice with specific examples depicted as facs dot plots. **(C)** Graphical representation of lesser percentages of splenic CD3+CD4+ and CD3+CD8+ T cells in *L. donovani* infected H (Wnt5A+/-) mice as compared to the controls (W: Wnt5A+/+) with examples. Data are presented as mean ± SEM. Statistical analysis was performed with the unpaired t-test. Significance was annotated as follows: *p ≤ 0.05, **p ≤ 0.005, ns, not significant, n=5 to 6 (per group).

contain the disease by restraining *L. donovani* infection and disease progression as revealed by the low liver and spleen LDU counts (**Figure 4**), low incidence of splenomegaly and liver granuloma (**Figures S3, S4**), and high frequency of organized

splenic white pulp (**Figure 5**) in the rWnt5A treated infected mice as compared to the corresponding controls.

Wnt5A mediated blockade in disease progression in experimental animals correlated with CD4/CD8 T cell activation
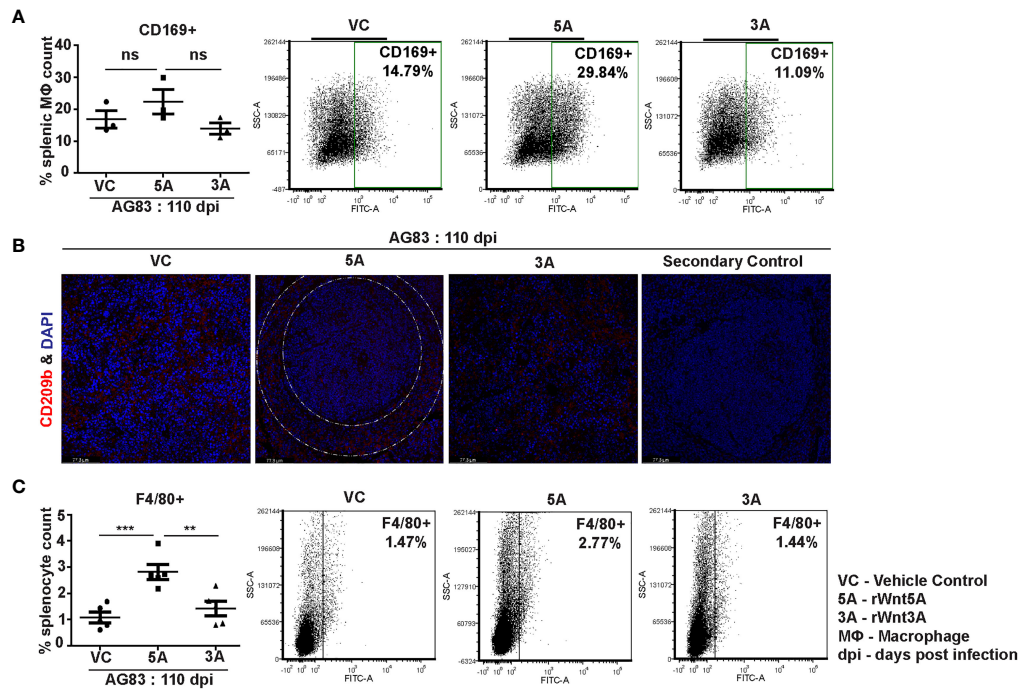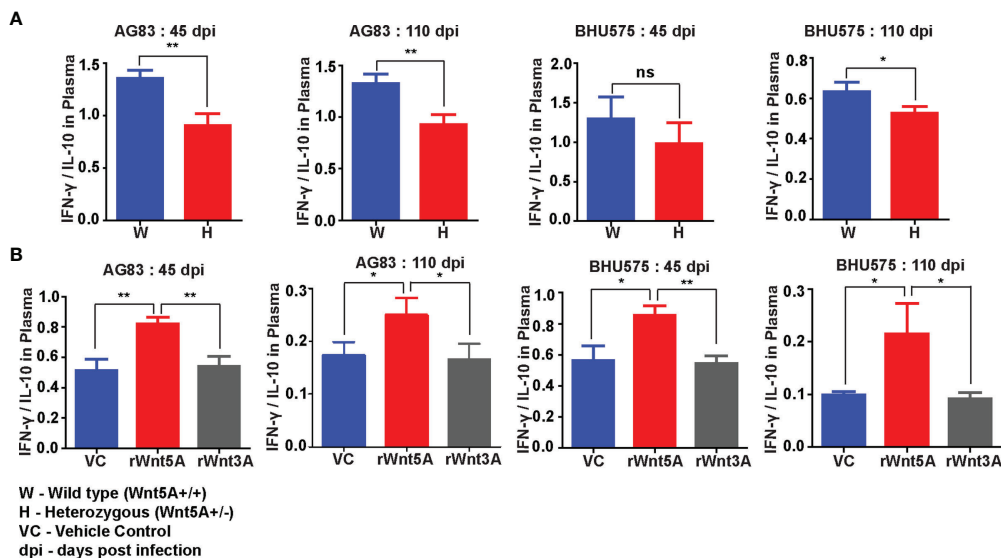
FIGURE 7 | rWnt5A supports preservation of splenic macrophages after *L. donovani* infection. **(A)** Graphical representation of increased percentage of CD169$^+$ splenic marginal metallophillic macrophages associated with rWnt5A treatment as compared to controls, with representative examples. **(B)** Preservation of CD209b$^+$ (in red) splenic marginal zone macrophages (marginal zone area denoted by white dashed concentric lines) in association with treatment of rWnt5A, but not rWnt3A or VC, as revealed by confocal microscopy (under 40X objective/oil immersion). DAPI stain represents nucleus. **(C)** Increased percentage of F4/80$^+$ macrophages in rWnt5A set as compared to vc and rWnt3A treated set, with representative examples. Statistical analysis was performed with the unpaired t-test. Data are presented as mean ± SEM. Significance was annotated as follows: **$p \leq 0.005$, ***$p \leq 0.0005$, ns, not significant, n=3 to 5 (per group).

as evident from the higher percentages of IFN-γ and GrB positive CD4 and CD8 T cells in the spleens of rWnt5A treated mice than those of the controls (**Figure 6**). The direct correlation between Wnt5A assisted IFN-γ response and decreased parasite numbers in our study is in accordance with other independent observations related to IFN-γ mediated inhibition of *L. donovani* infection (39, 40). The Wnt5A–IFN-γ connection is also in compliance with our previous observation related to Wnt5A mediated regulation of IFN-γ secretion (7). Wnt5A mediated disease suppression in infected animals was, furthermore, associated with an increased percentage of splenic red pulp (F4/80$^+$) and white pulp (CD169$^+$) macrophages along with the preservation of marginal zone (CD209b$^+$) macrophages, as compared to the controls (**Figure 7**). The prevalence of activated IFN-γ$^+$ T cells and almost conserved splenic organization linked with Wnt5A treatment of infected animals correlated with higher plasma IFN-γ/IL-10 ratio as compared to the corresponding controls (**Figure 8**), suggesting the possibility of restriction of IL-10 mediated disease exacerbation in the backdrop of a prevailing IFN-γ response (41). Wnt5A treatment prior to infection also correlated with slightly low plasma levels of IL-4 (**Figure S7**), which has been reported to worsen the disease outcome (42). However, in view of several other reports related to the uncertain status of IL-4 in the context of

visceral leishmaniasis (43–45), the significance of the Wnt5A-IL-4 connection in our study is unclear at present.

Previous findings from *in vitro* studies indicated that Wnt5A induced ROS and alteration of actin dynamics contributes to the reduction of parasite burden in *L. donovani* infected macrophages (19). In compliance with previous reports, we demonstrated Wnt5A dependent augmented ROS, which could be contributed by both red pulp and white pulp macrophages in the spleens of *L. donovani* infected mice (**Figures S8A, B**). In addition, we also demonstrated Wnt5A dependent increase in iNOS expression in parasite - infected macrophages as an attribute to Wnt5A mediated parasite killing (**Figures S8D, E**) (46). **Figure S9** explicitly depicts the disruption of supposedly protective actin ring niches that are usually present around the parasite containing vacuoles in *L. donovani* infected peritoneal macrophages, through activation of Wnt5A signaling. Such remodeling of cytoskeletal actin in the macrophages of the red pulp (F4/80$^+$) and white pulp (CD169$^+$ and CD209b$^+$), which are preserved by Wnt5A signaling in infected animals (**Figure 7**), could lead to inhibition in actin niche formation around parasitophorous vacuoles and destruction of parasites. The marginal zone (CD209b) and marginal metallophillic (CD169) macrophages, moreover could aid in the presentation

FIGURE 8 | rWnt5A promotes a IFN-γ/proinflammatory bias cytokine during *L. donovani* infection. **(A)** Graphical representation of higher IFN-γ/IL-10 ratio in the blood plasma of AG83 and BHU575 infected Wnt5A+/+ (W) mice as compared to Wnt5A+/- (H) mice. **(B)** rWnt5A treatment before AG83 or BHU575 infection correlates with higher plasma IFN-γ/IL-10 in comparison to rWnt3A or VC treatment. Statistical analysis was performed with the unpaired t-test. Data are presented as mean ± SEM. Significance was annotated as follows: $*p \leq 0.05$, $**p \leq 0.005$, ns, not significant, n=6 (per group).

of dead parasite fragments to T cells leading to T cell activation and cytokine secretion (32, 34–36). Such intercellular coordination during infection could lead to sustained activation of macrophages and T cells targeted toward parasite clearance.

Overall, our animal experiments indicate that Wnt5A signaling reduces susceptibility to *L. donovani* infection and progression of visceral leishmaniasis at least partly through the maintenance of functional macrophages and T cells, elaboration of a disease limiting cytokine profile and preservation of splenic architecture. In a very preliminary study comprising only a limited number of blood plasma samples collected from healthy individuals and patients with VL or PKDL (Post Kala-azar Dermal Leishmaniasis), we in fact noted, that healthy individuals and most of the patients either under treatment with miltefosine or with no symptom of VL had higher level of Wnt5A in their plasma than those with symptomatic VL or PKDL. (**Table S1**, **Figure S10**). It will thus be important to examine the relevance of Wnt5A in relation to VL/PKDL using an appropriate number of healthy volunteers and test subjects with a clear history of the disease. Furthermore, future experiments directed toward the use of recombinant Wnt5A as a prophylactic or therapeutic agent may prove useful for restricting progression of the refractory disease that is poorly managed by the currently administered drugs.

DATA AVAILABILITY STATEMENT

The raw data supporting the conclusions of this article will be made available by the authors, without undue reservation.

ETHICS STATEMENT

The use of animals was approved by the Animal Ethics Committee of IICB. The identification numbers of the approved projects are IICB/AEC/Meeting/2016/Aug, IICB/AEC/Meeting/Aug/2018/4 and IICB/AEC/Meeting/Sep/2019/1. Collection of blood from human volunteers during May 2019 was approved by the Ethical Committee of Human Subjects (dated February 10, 2018). Written informed consent to participate in this study was provided by the participants or their legal guardian.

AUTHOR CONTRIBUTIONS

MS designed research, analyzed data, and wrote the paper. SM performed research, intellectually contributed to research design, analyzed data, and assisted in writing the paper. AC was involved in initiating the project. SKM performed EM experiments. SR and AD helped in histology experiments and fieldwork.

FUNDING

ACKNOWLEDGMENTS

SUPPLEMENTARY MATERIAL

The Supplementary Material for this article can be found online at: https://www.frontiersin.org/articles/10.3389/fimmu.2022.818266/full#supplementary-material

REFERENCES

1. Kaye P, Scott P. Leishmaniasis: Complexity at the Host–Pathogen Interface. *Nat Rev Microbiol* (2011) 9:604–15. doi: 10.1038/nrmicro2608
2. Olivier M, Gregory DJ, Forget G. Subversion Mechanisms by Which Leishmania Parasites Can Escape the Host Immune Response: A Signaling Point of View. *Clin Microbiol Rev* (2005) 18:293–305. doi: 10.1128/CMR.18.2.293-305.2005
3. Chappuis F, Sundar S, Hailu A, Ghalib H, Rijal S, Peeling RW, et al. Visceral Leishmaniasis: What are the Needs for Diagnosis, Treatment and Control? *Nat Rev Microbiol* (2007) 5:873–82. doi: 10.1038/nrmicro1748
4. Alves F, Bilbe G, Blesson S, Goyal V, Monnerat S, Mowbray C, et al. Recent Development of Visceral Leishmaniasis Treatments: Successes, Pitfalls, and Perspectives. *Clin Microbiol Rev* (2018) 31:e00048–18. doi: 10.1128/CMR.00048-18
5. Ponte-Sucre A, Gamarro F, Dujardin J-C, Barrett MP, López-Vélez R, García-Hernández R, et al. Drug Resistance and Treatment Failure in Leishmaniasis: A 21st Century Challenge. *PloS Negl Trop Dis* (2017) 11:e0006052. doi: 10.1371/journal.pntd.0006052
6. Maiti G, Naskar D, Sen M. The Wingless Homolog Wnt5a Stimulates Phagocytosis But Not Bacterial Killing. *Proc Natl Acad Sci U.S.A.* (2012) 109:16600–5. doi: 10.1073/pnas.1207789109
7. Naskar D, Maiti G, Chakraborty A, Roy A, Chattopadhyay D, Sen M. Wnt5a–Rac1–NF-κb Homeostatic Circuitry Sustains Innate Immune Functions in Macrophages. *J Immunol* (2014) 192:4386–97. doi: 10.4049/jimmunol.1302817
8. Jati S, Kundu S, Chakraborty A, Mahata SK, Nizet V, Sen M. Wnt5A Signaling Promotes Defense Against Bacterial Pathogens by Activating a Host Autophagy Circuit. *Front Immunol* (2018) 9:679. doi: 10.3389/fimmu.2018.00679
9. Jati S, Sengupta S, Sen M. Wnt5A-Mediated Actin Organization Regulates Host Response to Bacterial Pathogens and Non-Pathogens. *Front Immunol* (2021) 11:628191. doi: 10.3389/fimmu.2020.628191
10. Jati S, Sarraf TR, Naskar D, Sen M. Wnt Signaling: Pathogen Incursion and Immune Defense. *Front Immunol* (2019) 10:2551. doi: 10.3389/fimmu.2019.02551
11. Veeman MT, Axelrod JD, Moon RT. A Second Canon: Functions and Mechanisms of β-Catenin-Independent Wnt Signaling. *Dev Cell* (2003) 5:367–77. doi: 10.1016/S1534-5807(03)00266-1
12. Minami Y, Oishi I, Endo M, Nishita M. Ror-Family Receptor Tyrosine Kinases in Noncanonical Wnt Signaling: Their Implications in Developmental Morphogenesis and Human Diseases. *Dev Dyn* (2010) 239:1–15. doi: 10.1002/dvdy.21991
13. Schulte G, Bryja V. The Frizzled Family of Unconventional G-Protein-Coupled Receptors. *Trends Pharmacol Sci* (2007) 28:518–25. doi: 10.1016/j.tips.2007.09.001
14. Nishita M, Itsukushima S, Nomachi A, Endo M, Wang Z, Inaba D, et al. Ror2/Frizzled Complex Mediates Wnt5a-Induced AP-1 Activation by Regulating Dishevelled Polymerization. *Mol Cell Biol* (2010) 30:3610–9. doi: 10.1128/MCB.00177-10
15. *Wnt Signaling: A Common Theme in Animal Development*. Available at: http://genesdev.cshlp.org/content/11/24/3286.long (Accessed November 1, 2021).
16. Mikels AJ, Nusse R. Purified Wnt5a Protein Activates or Inhibits β-Catenin–TCF Signaling Depending on Receptor Context. *PloS Biol* (2006) 4:e115. doi: 10.1371/journal.pbio.0040115
17. Gon H, Fumoto K, Ku Y, Matsumoto S, Kikuchi A. Wnt5a Signaling Promotes Apical and Basolateral Polarization of Single Epithelial Cells. *Mol Biol Cell* (2013) 24:3764–74. doi: 10.1091/mbc.E13-07-0357
18. Schlessinger K, McManus EJ, Hall A. Cdc42 and Noncanonical Wnt Signal Transduction Pathways Cooperate to Promote Cell Polarity. *J Cell Biol* (2007) 178:355–61. doi: 10.1083/jcb.200701083
19. Chakraborty A, Kurati SP, Mahata SK, Sundar S, Roy S, Sen M. Wnt5a Signaling Promotes Host Defense Against Leishmania Donovani Infection. *J Immunol* (2017) 199:992–1002. doi: 10.4049/jimmunol.1601927
20. Katakura K. An Experimental Challenge Model of Visceral Leishmaniasis by Leishmania Donovani Promastigotes in Mice. *Parasitol Int* (2016) 65:603–6. doi: 10.1016/j.parint.2016.03.008
21. Feldman AT, Wolfe D. "Tissue Processing and Hematoxylin and Eosin Staining.,". In: CE Day, editor. *Histopathology: Methods and Protocols. Methods in Molecular Biology*. New York, NY: Springer (2014). p. 31–43. doi: 10.1007/978-1-4939-1050-2_3
22. Santana CC, Vassallo J, De Freitas LAR, Oliveira GGS, Pontes-De-Carvalho LC, Dos-Santos WLC. Inflammation and Structural Changes of Splenic Lymphoid Tissue in Visceral Leishmaniasis: A Study on Naturally Infected Dogs. *Parasit Immunol* (2008) 30:515–24. doi: 10.1111/j.1365-3024.2008.01051.x
23. Scanziani E. "Immunohistochemical Staining of Fixed Tissues.,". In: R Miles, R Nicholas, editors. *Mycoplasma Protocols. Methods in Molecular BiologyTM*. Totowa, NJ: Humana Press (1998). p. 133–40. doi: 10.1385/0-89603-525-5:133
24. Joshi S, Yu D. "Chapter 8 - Immunofluorescence.,". In: M Jalali, FYL Saldanha, M Jalali, editors. *Basic Science Methods for Clinical Researchers*. Boston: Academic Press (2017). p. 135–50. doi: 10.1016/B978-0-12-803077-6.00008-4
25. Anam K, Afrin F, Banerjee D, Pramanik N, Guha SK, Goswami RP, et al. Differential Decline in Leishmania Membrane Antigen-Specific Immunoglobulin G (IgG), IgM, IgE, and IgG Subclass Antibodies in Indian Kala-Azar Patients After Chemotherapy. *Infect Immun* (1999) 67:6663–9. doi: 10.1128/IAI.67.12.6663-6669.1999
26. Rodrigues V, Cordeiro-da-Silva A, Laforge M, Silvestre R, Estaquier J. Regulation of Immunity During Visceral Leishmania Infection. *Parasit Vectors* (2016) 9:118. doi: 10.1186/s13071-016-1412-x
27. Silva-O'Hare J, Oliveira IS de, Klevorn T, Almeida VA, Oliveira GGS, Atta AM, et al. Disruption of Splenic Lymphoid Tissue and Plasmacytosis in Canine Visceral Leishmaniasis: Changes in Homing and Survival of Plasma Cells. *PloS One* (2016) 11:e0156733. doi: 10.1371/journal.pone.0156733
28. d'El-Rei Hermida M, de Melo CVB, Lima IDS, de Sa Oliveira GG, Dos-Santos WLC. Histological Disorganization of Spleen Compartments and Severe Visceral Leishmaniasis. *Front Cell Infect Microbiol* (2018) 8:394. doi: 10.3389/fcimb.2018.00394
29. Salguero FJ, Garcia-Jimenez WL, Lima I, Seifert K. Histopathological and Immunohistochemical Characterisation of Hepatic Granulomas in Leishmania Donovani-Infected BALB/c Mice: A Time-Course Study. *Parasit Vectors* (2018) 11:73. doi: 10.1186/s13071-018-2624-z
30. Terrazas C, Varikuti S, Oghumu S, Steinkamp HM, Ardic N, Kimble J, et al. Ly6Chi Inflammatory Monocytes Promote Susceptibility to Leishmania Donovani Infection. *Sci Rep* (2017) 7:14693. doi: 10.1038/s41598-017-14935-3
31. van Loosdregt J, Coffer PJ. The Role of WNT Signaling in Mature T Cells: T Cell Factor Is Coming Home. *J Immunol* (2018) 201:2193–200. doi: 10.4049/jimmunol.1800633
32. Ghosh MC, Collins GD, Vandanmagsar B, Patel K, Brill M, Carter A, et al. Activation of Wnt5A Signaling is Required for CXC Chemokine Ligand 12–Mediated T-Cell Migration. *Blood* (2009) 114:1366–73. doi: 10.1182/blood-2008-08-175869

33. Mastelaro de Rezende M, Zenker Justo G, Julian Paredes-Gamero E, Gosens R. Wnt-5a/B Signaling in Hematopoiesis Throughout Life. *Cells* (2020) 9:E1801. doi: 10.3390/cells9081801

34. van Dinther D, Veninga H, Iborra S, Borg EGF, Hoogterp L, Olesek K, et al. Functional CD169 on Macrophages Mediates Interaction With Dendritic Cells for CD8+ T Cell Cross-Priming. *Cell Rep* (2018) 22:1484–95. doi: 10.1016/j.celrep.2018.01.021

35. Backer R, Schwandt T, Greuter M, Oosting M, Jüngerkes F, Tüting T, et al. Effective Collaboration Between Marginal Metallophilic Macrophages and CD8+ Dendritic Cells in the Generation of Cytotoxic T Cells. *Proc Natl Acad Sci U.S.A.* (2010) 107:216–21. doi: 10.1073/pnas.0909541107

36. Borges da Silva H, Fonseca R, Pereira RM, Cassado A dos A, Álvarez JM, D'Império Lima MR. Splenic Macrophage Subsets and Their Function During Blood-Borne Infections. *Front Immunol* (2015) 6:480. doi: 10.3389/fimmu.2015.00480

37. Samant M, Sahu U, Pandey SC, Khare P. Role of Cytokines in Experimental and Human Visceral Leishmaniasis. *Front Cell Infect Microbiol* (2021) 11:624009. doi: 10.3389/fcimb.2021.624009

38. Bhowmick S, Ravindran R, Ali N. IL-4 Contributes to Failure, and Colludes With IL-10 to Exacerbate Leishmania Donovani Infection Following Administration of a Subcutaneous Leishmanial Antigen Vaccine. *BMC Microbiol* (2014) 14:8. doi: 10.1186/1471-2180-14-8

39. Hockertz S, Franke G, Paulini I, Lohmann-Matthes ML. Immunotherapy of Murine Visceral Leishmaniasis With Murine Recombinant Interferon-Gamma and MTP-PE Encapsulated in Liposomes. *J Interferon Res* (1991) 11:177–85. doi: 10.1089/jir.1991.11.177

40. Sundar S, Murray HW. Effect of Treatment With Interferon-γ Alone in Visceral Leishmaniasis. *J Infect Dis* (1995) 172:1627–9. doi: 10.1093/infdis/172.6.1627

41. *Balance of IL-10 and Interferon-γ Plasma Levels in Human Visceral Leishmaniasis: Implications in the Pathogenesis | BMC Infectious Diseases | Full Text*. Available at: https://bmcinfectdis.biomedcentral.com/articles/10.1186/1471-2334-5-113 (Accessed December 28, 2021).

42. Zwingenberger K, Harms G, Pedrosa C, Omena S, Sandkamp B, Neifer S. Determinants of the Immune Response in Visceral Leishmaniasis: Evidence for Predominance of Endogenous Interleukin 4 Over Interferon-Gamma Production. *Clin Immunol Immunopathol* (1990) 57:242–9. doi: 10.1016/0090-1229(90)90038-r

43. Lehmann J, Enssle K-H, Lehmann I, Emmendorfer A, Lohmann-Matthes M-L. The Capacity to Produce IFN-Gamma Rather Than the Presence of Interleukin-4 Determines the Resistance and the Degree of Susceptibility to Leishmania Donovani Infection in Mice. *J Interferon Cytokine Res* (2000) 20:63–77. doi: 10.1089/107999000312748

44. Satoskar A, Bluethmann H, Alexander J. Disruption of the Murine Interleukin-4 Gene Inhibits Disease Progression During Leishmania Mexicana Infection But Does Not Increase Control of Leishmania Donovani Infection. *Infect Immun* (1995) 63:4894–9. doi: 10.1128/iai.63.12.4894-4899.1995

45. Basu R, Bhaumik S, Haldar Ak, Naskar K, De T, Dana Sk, et al. Hybrid Cell Vaccination Resolves Leishmania Donovani Infection by Eliciting a Strong CD8+ Cytotoxic T-Lymphocyte Response With Concomitant Suppression of Interleukin-10 (IL-10) But Not IL-4 or IL-13. *Infect Immun* (2007) 75:5956–66. doi: 10.1128/IAI.00944-07

46. Murray HW, Nathan CF. Macrophage Microbicidal Mechanisms *In Vivo*: Reactive Nitrogen Versus Oxygen Intermediates in the Killing of Intracellular Visceral Leishmania Donovani. *J Exp Med* (1999) 189:741–6. doi: 10.1084/jem.189.4.741